Journal of Materials Chemistry B

Accepted Manuscript

ROYAL SOCIETY OF CHEMISTRY

www.rsc.org/materialsB

Journal of Materials Chemistry B

ARTICLE

Delivery of AIB1 siRNA by Ca^{2+}/PEI/Heparin Composite Nanoparticles Effectively Inhibits Growth of Human Breast Cancer

Cite this: DOI: 10.1039/x0xx00000x

Received 23th December 2014,
Accepted 00th January 2012

DOI: 10.1039/x0xx00000x

www.rsc.org/

T.Y. Cheang,[a,#] Z.H. Xing,[b,#] Z.L. Li,[c,#] H.Y. Zhou,[d] J.H. Wei,[e] X. Zhou,[f] A.W. Xu,[f,*] Y. Lin,[a,*] S.M. Wang[a,*]

Here, a novel carrier fabricated by interaction of negatively charged heparin and positively charged PEI and Ca^{2+} was investigated to deliver AIB1 siRNA to breast cancer cells both *in vitro* and *in vivo*. The Ca^{2+}/PEI/Heparin nanoparticles were prepared by simply mixed of heparin, PEI and $CaCl_2$ aqueous solution. Heparin in the Ca^{2+}/PEI/Heparin nanoparticles (40.9% heprarin, w/w) decreased the cytotoxicity of PEI. According to the MTT assay, Ca^{2+}/PEI/Heparin NPs is superior to commercial Lipofectamine 2000 considering the safety. The Ca^{2+}/PEI/Heparin NPs are able to deliver siAIB1 into breast cancer cells as effectively as Lipofectamine 2000 both *in vitro* and *in vivo*. The *in vivo* experiment also indicated that NF-κB/BCL-2 signal pathway might be the downstream signal pathway of AIB1 in regulating breast cancer proliferation and progression.

Keywords: human breast cancer, Ca^{2+}/PEI/Heparin Composite Nanoparticles, siRNA, gene therapy

Introduction

Gene therapy, introducing genetic materials into cells to treat diseases by modifying gene expression, offers a novel alternative to conventional therapy in cancer management. Efficient delivery of therapeutic genes into target cells or organs without causing any toxic effect remains a key component in gene therapy. It has been widely accepted that an ideal gene delivery system should be target-specific, biodegradable, nontoxic, non-immunogenic and stable during storage.[1] However, developing such a system remains to be the biggest challenge.

Nonviral polymer carriers are considered superior to viral gene delivery systems, largely because of easy preparation and reduced risk of immune response.[2] Polyethyleneimine (PEI), a commonly used synthetic cationic polymer for gene delivery,[3-6] is known to have high transfection efficiency both *in vitro* and *in vivo*. However, PEI often shows higher toxicity compared with viral vectors.[7-9] Especially for 25 kDa branched PEI, which is confirmed to be less efficient and more toxic than linear PEI.[10, 11] As a natural and safe biomaterial, heparin is widely used in the clinical setting, [12] which can act as anticoagulation drug to inhibit of venous embolism. The high negative charge density of heparin contributes to its strong electrostatic interaction with cationic molecules.[13] In the past decade, heparin and cationic protamine formed nanocomplexes were used to label cells without short- or long-term toxicity [14] and facilitate intracellular drug delivery.[15, 16] Previous work showed that heparin/PEI nanoparticles with an average diameter of 171 nm can transfect EGFP plasmid DNA into Hela and 293T cells with low cytotoxicity.[17]

In this study, negatively charged heparin was used to crosslink with positively charged branched PEI and Ca^{2+} ions to form Ca^{2+}/PEI/Heparin nanoparticles (Ca^{2+}/PEI/Heparin NPs). The Ca^{2+}/PEI/Heparin NPs with small size (about 25 nm in average diameter) and highly positive surface charge (ζ-potential +29.3 mV) were used in siRNA delivery both *in vitro* and *in vivo*, and its efficiency and safety were compared with the commercial lipid Lipofectamine 2000.

Results and discussion

Scanning electron microscopy (SEM) image and size analysis of Ca^{2+}/PEI/Heparin NPs.

The Ca^{2+}/PEI/Heparin NPs are spherical in shape and about 25 nm in diameter (Figure 1a). Without Ca^{2+}, PEI and heparin conjugated and fabricated micro-scale fibers (Figure 1b), suggesting that the Ca^{2+} ions play an important role in the shape formation of the

nanoparticles. The average dimension of the suspended nanoparticles was measured by means of a dynamic light scattering (DLS) apparatus. Compare the DLS data with the SEM image, a certain degree of NP agglomeration can be found under the conditions (Figure 2). But the scale of large NP and small aggregates are still under 100 nm (average diameter: 80.3 nm).

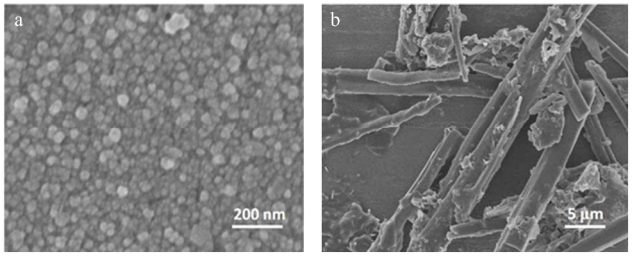

Figure 1. Scanning electron microscopy images of (a) the Ca^{2+}/PEI/Heparin NPs, and (b) PEI/Heparin.

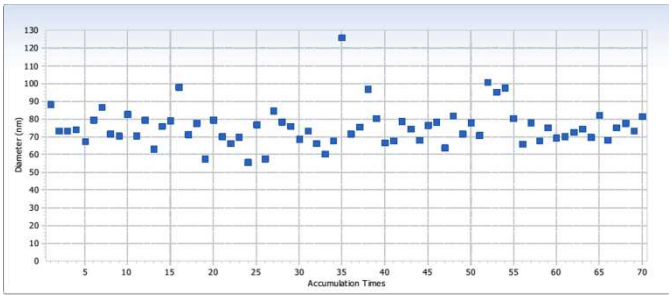

Figure 2. Size analysis with dynamic light scattering (DLS).

Fourier transform infrared (FTIR) spectra and Energy dispersive X-ray spectroscopy (EDS) spectrum of Ca^{2+}/PEI/Heparin NPs.

IR spectra of PEI (Figure 3) showed that the 1592 and 1646 cm^{-1} bands are attributed to the bending vibrations of $–NH_2$. In the spectra of Ca^{2+}/PEI/Heparin NPs, the two bands are overlapped with the peak of $–NH_2$ in heparin at 1620 cm^{-1}.[18] Characteristic peaks of heparin appeared at 891 and 942 cm^{-1} can be found in both the IR spectra of heparin and Ca^{2+}/PEI/Heparin NPs, the existence of heparin in the NPs is further confirmed. Informed from the producer, the content of sulfur in heparin is 10% at mass ratio.[19] According to the EDS analysis, the mass ratio of heparin in the final product is evaluated to be 40.9%.

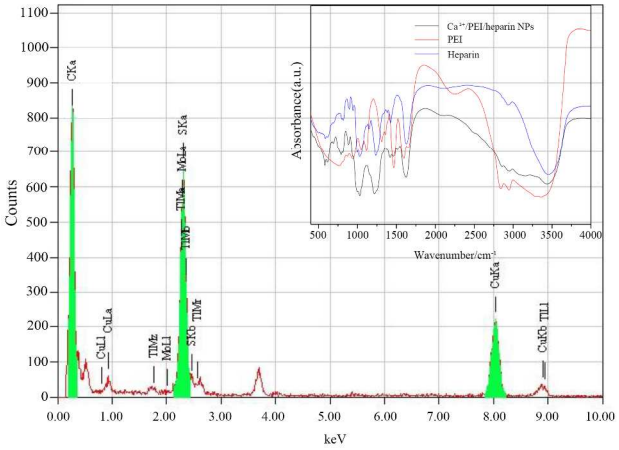

Figure 3. Fourier transform infrared (FTIR) spectra and Energy dispersive X-ray spectroscopy (EDS) spectrum of Ca^{2+}/PEI/Heparin NPs. The inset graph is IR spectra of Ca^{2+}/PEI/Heparin NPs, PEI and Heparin.

siRNA-binding efficiency and cytotoxicity of Ca^{2+}/PEI/Heparin NPs.

siRNA-binding efficiency was detected by electrophoretic mobility of the siRNA within agarose gel. The mass ratio of the Ca^{2+}/PEI/Heparin NPs to siRNA ranged from 1:1 to 100:1. As shown in Figure 4a, incubation of increasing amounts of Ca^{2+}/PEI/Heparin NPs with siRNA resulted in a decrease of siRNA mobility. When the Ca^{2+}/PEI/Heparin NPs and siRNA were mixed at the mass ratio of 50:1, Ca^{2+}/PEI/Heparin NPs completely retarded the migration of siRNA. This ratio was considered as the optimal mass ratio, which is consistent with our previous study.[20] ζ-potential measurements showed that the Ca^{2+}/PEI/Heparin NPs carried a positive surface potential of +29.3 mV, which contributes to the electrostatic interaction with negatively charged siRNAs during forming Ca^{2+}/PEI/Heparin NPs /siRNA complex.

The cytotoxicity of Ca^{2+}/PEI/Heparin NPs was determined by MTT assays. Cells were treated with Ca^{2+}/PEI/Heparin NPs/siNC complexes of different concentrations. As shown in Figure 4b, even at the highest concentration (150 μg/mL), Ca^{2+}/PEI/Heparin NPs/siNC showed little cytotoxicity to the cells, indicating heparin greatly reduced the cytotoxicity of 25-kDa PEI.[21] In contrast, Lipofectamine 2000 showed significant cytotoxicity at the effective dose recommended by the manufacturer. This result is suggested to be a potential siRNA delivery system, as the Ca^{2+}/PEI/Heparin NPs is superior to Lipofectamine 2000 considering the safety.

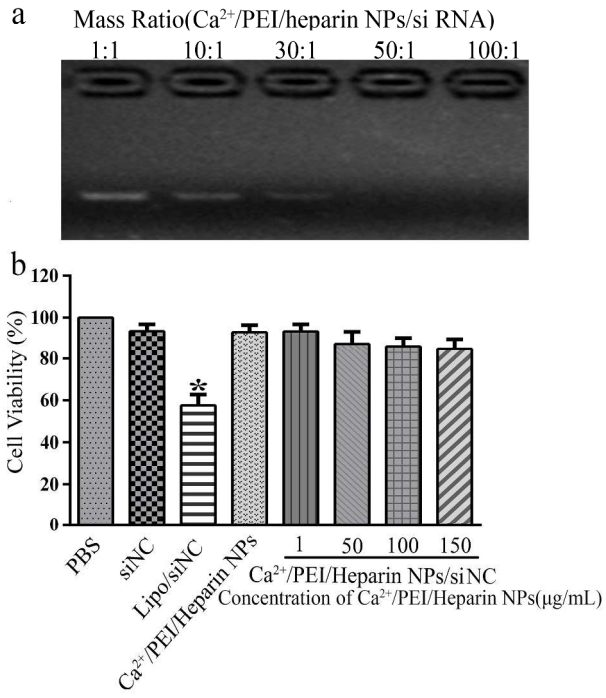

Figure 4. siRNA-binding efficiency and cytotoxicity of Ca^{2+}/PEI/Heparin NPs. (a) Binding ability of Ca^{2+}/PEI/Heparin to siRNA at different ratios of complex detected by the gel retardation assay. (b) MTT assay was performed to assess cell cytotoxicity of Ca^{2+}/PEI/Heparin NPs. siNC, negative control small interfering RNA; lipo, Lipofectamine 2000. The graph represents as the mean ± SD of three independent experiments.*$P < 0.05$ vs PBS.

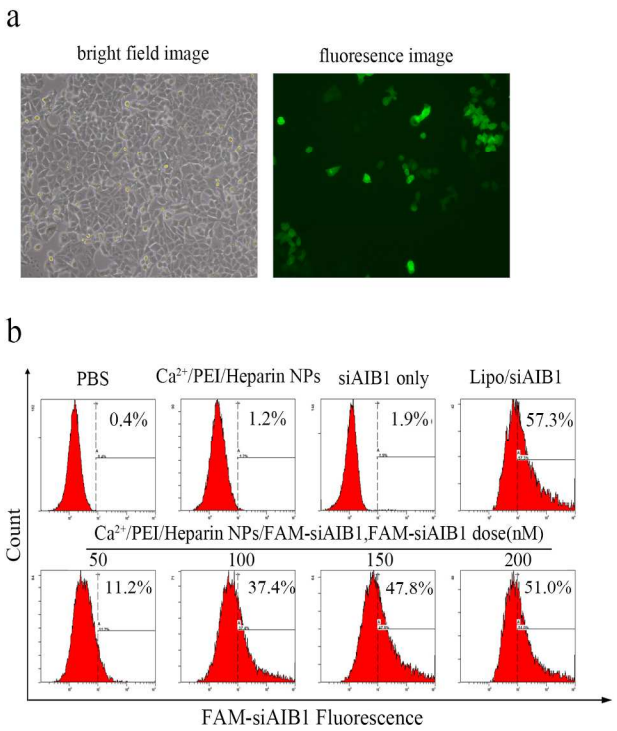

Figure 5. The transfection efficiency of Ca^{2+}/PEI/Heparin NPs delivered siAIB1 into MCF-7 cells. (a) Inverted fluorescence microscopy images showing FAM-siRNA fluorescence 6 h after transfection. (b) Percentages of fluorescent cells measured by flow cytometry.

Transfection efficiency

To investigate the transfection efficiency of siRNA into human breast cancer cells, the uptake of Ca^{2+}/PEI/Heparin NPs/FAM-siAIB1 complexes by MCF-7 cells was analyzed by an inverted fluorescence microscope. As shown in Figure 5, FAM-siAIB1 was observed within the MCF-7 cells after 6 h incubation, indicating the internalization of Ca^{2+}/PEI/Heparin NPs.

Ca^{2+}/PEI/Heparin NPs/FAM-siAIB1 was incubated with MCF-7 cells, for 6 h, and the cells were analyzed by flow cytometry after quenching the extracellular fluorescence with trypan blue solution to further understand the intracellular behavior of the nanoparticles loaded with siRNA. As shown in Figure 5, the percentage of fluorescent cells transfected with Ca^{2+}/PEI/Heparin NPs/FAM-siAIB1 complexes increased with higher amount of FAM-siAIB1. Notably, when the dose of FAM-siAIB1 increase to 150 nM, cells incubated with Ca^{2+}/PEI/Heparin NPs/FAM-siAIB1 complexes exhibited similar transfection efficiency compared to cells incubated with Lipofectamine 2000/FAM-siAIB1 complexes. The concentration of 200 nM did not improve the transfection efficiency significantly. Thus, the optimal concentration for siRNA delivery by Ca^{2+}/PEI/Heparin NPs in MCF-7 cells was 150 nM. These results demonstrated that Ca^{2+}/PEI/Heparin NPs are able to deliver siAIB1 into MCF-7 cells as effectively as Lipofectamine 2000.

We validated the transfection efficiency of siRNA into human breast cancer cells on SK-BR-3 cells and MAD-MB-231cells(Supplementary Figure 1) other than MCF-7 cells. And they showed the similar trend with that in MCF-7 cells. When the dose of FAM-siAIB1 increase to 150 nM, cells incubated with Ca^{2+}/PEI/Heparin NPs/FAM-siAIB1 complexes exhibited similar transfection efficiency compared to cells incubated with Lipofectamine 2000/FAM-siAIB1 complexes. The concentration of 200 nM did not improve the transfection efficiency significantly. Thus, the optimal concentration for siRNA delivery by Ca^{2+}/PEI/Heparin NPs in MCF-7 cells, SK-BR-3 cells and MAD-MD-231 cells was 150 nM. These results confirmed that Ca^{2+}/PEI/Heparin NPs are able to deliver siAIB1 into MCF-7 cells as effectively as Lipofectamine 2000.

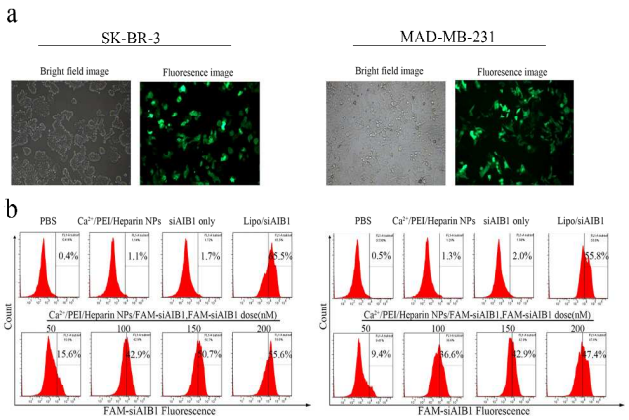

Supplementary Figure 1. The transfection efficiency of Ca^{2+}/PEI/Heparin NPs delivered siAIB1 into SK-BR-3 cells and MAD-MB-231 cells. (a) Inverted fluorescence microscopy images showing FAM-siRNA fluorescence 6 h after transfection. (b) Percentages of fluorescent cells measured by flow cytometry.

Intracellular distribution of FAM-labeled siRNA

MCF-7 cells were transfected with Ca^{2+}/PEI/Heparin NPs/FAM-siRNA for 24 h to evaluate the endosomal escaping behavior. The nucleis were stained with DAPI, and Lyso-Traker Red was used to label and track the presence of lysosomes. As shown in Figure 6, FAM-siAIB1 fluorescence were punctately distributed in the MCF-7 cell cytoplasm and the periphery of the nuclei, suggesting FAM-siAIB1 was effectively delivered into cells. The presence of PEI and Ca^{2+} can induce the endosome destabilization and enhance the endosomal escaping efficacy.[20, 22] This phenomenon of endosomal escape of Ca^{2+}/PEI/Heparin NPs is well correlated with the result of the following AIB1 knockdown experiment.

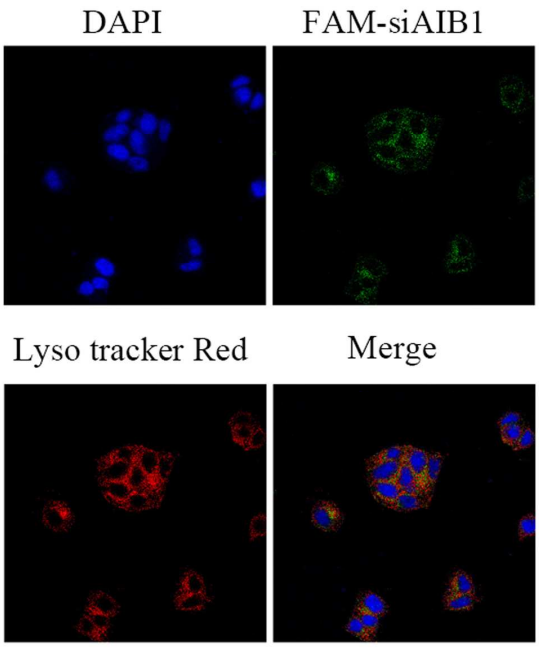

Figure 6. The intracellular distribution of Ca^{2+}/PEI/Heparin NPs in MCF-7 cells. Lysosomes were stained with Lyso-Tracker Red (red). FAM-siAIB1 was labled in green. Cell nuclei were stained with DAPI (blue).

Cell proliferation, apoptosis, and cell cycle analyses

AIB1 mRNA and protein levels were measured by real-time PCR and Western blotting respectively to confirm the knockdown of AIB1 in MCF-7 cells. As shown in Figure 7a, the expression of AIB1 protein decreased in a dose-dependent manner. Consistently, AIB1 mRNA levels decreased in a dose-dependent manner in Ca^{2+}/PEI/Heparin NPs/FAM-siAIB1 transfected cells, while the pattern was not observed in the Ca^{2+}/PEI/Heparin NPs/siNC transfected cells (Figure 7a). Taken together, these results indicate that the transfection of Ca^{2+}/PEI/Heparin NPs/siAIB1 complexes can efficiently knockdown AIB1 at both mRNA and protein levels in MCF-7 cells.

Next, the effect of Ca^{2+}/PEI/Heparin NPs/siAIB1 complexes on the proliferation of MCF-7 cells was evaluated by MTT assay, absorbance at 490 nm. As shown in Figure. 7b, the proliferation of MCF-7 cells transfected with Ca^{2+}/PEI/Heparin NPs/siAIB1 complexes were significantly lower than that of the control group. In addition, Ca^{2+}/PEI/Heparin NPs/siAIB1 complexes inhibited the cell proliferation in a concentration-dependent manner. These results suggest that siAIB1 is involved in the proliferation of MCF-7 cells.

To further explore if Ca^{2+}/PEI/Heparin NPs/siAIB1 complexes would affect the cellular apoptosis, MCF-7 cells transfected with difference concentrations of Ca^{2+}/PEI/Heparin NPs/siAIB1 complexes were stained with Annexin V-FITC and propidium iodide (PI). As shown in Figure 7c, the percentage of apoptotic cells in the Ca^{2+}/PEI/Heparin NPs/siAIB1complexes (150 nM, 30.8%) transfected group is significantly higher than the cells transfected with control siRNA (siNC, 150nM, 5.9%), suggesting that apoptosis was due to AIB1 downregulation.

The Coulter DNA Prep Reagents Kit was used and the cell cycle progression was studied by flow cytometric analysis to analyze cell cycle distribution. As shown in Figure 7d, Ca^{2+}/PEI/Heparin NPs/siAIB1 markedly decreased the proportion of cells in S phase as compared with the control groups. When the siAIB1 dose increase to 150 nM, striking decrease of S phase cells (only 4.5% remained) was obtained.

Collectively, these results indicate that Ca^{2+}/PEI/Heparin NPs/siAIB1 treatment has profound anti-tumor effects as evidenced by inhibition of proliferation, induction of apoptosis and cell cycle arrest *in vitro*.

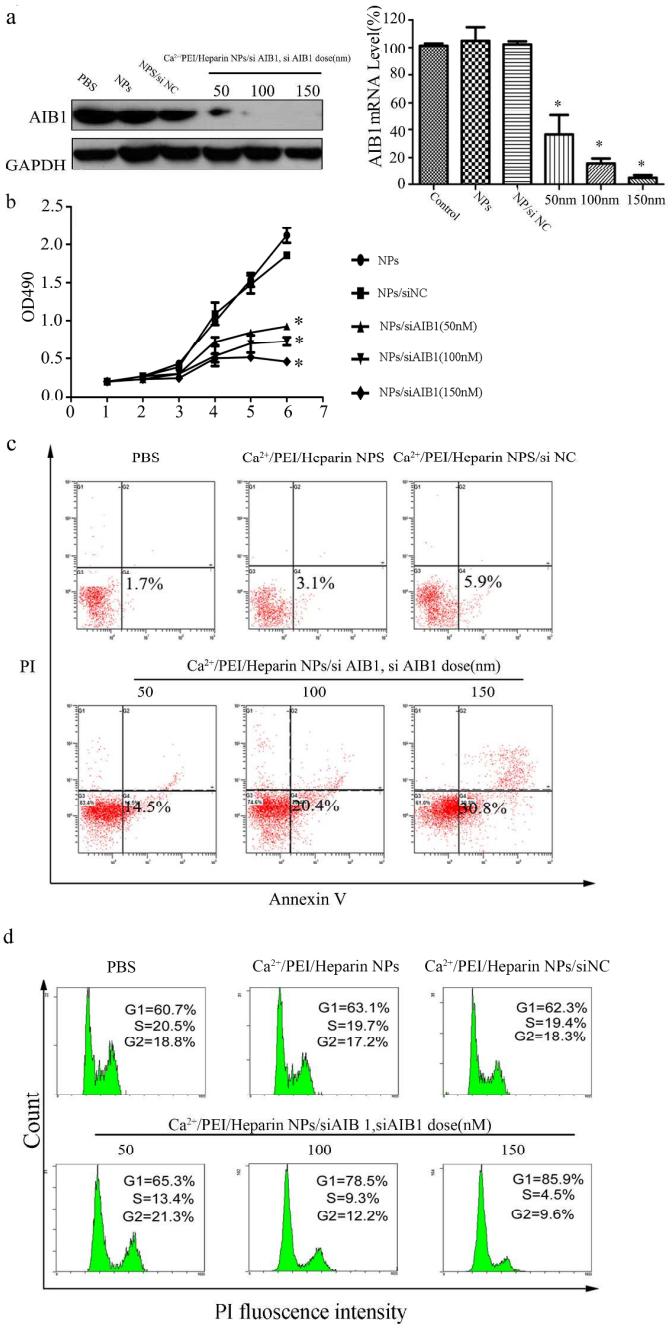

Figure 7. Knockdown of AIB1 mediated by Ca^{2+}/PEI/Heparin NPs transfection affected MCF-7 cells growth. (a) Ca^{2+}/PEI/Heparin NPs transfection significantly inhibited the expression levels of AIB1 protein and mRNA in MCF-7 cells. *$P < 0.05$ vs control. Effects of AIB1 down-regulation on cell viability (b), cell apoptosis (c) and cell cycle (d).

FAM-siAIB1 biodistribution in tumor tissues *in vivo*.

Ca^{2+}/PEI/Heparin NPs/siAIB1 was intratumorally injected into the subcutaneous xenograft of mice, and *in vivo* imaging technology was used to evaluate the tissue distribution of FAM-siAIB1. The FAM-siAIB1 dispersed in PBS solution was prepared as controls. As shown in Figure 8a, 0.5 h after the injection, the tumors injected with Ca^{2+}/PEI/Heparin NPs/FAM-siAIB1 exhibited stronger fluorescence intensity and larger fluorescence distribution area compared with the tumors injected with FAM-siAIB1 alone or PBS solution, indicating better penetrability of Ca^{2+}/PEI/Heparin NPs/FAM-siAIB1 into the tumor tissue. Furthermore, the fluorescence in the tumors transfected with Ca^{2+}/PEI/Heparin NPs/FAM-siAIB1 lasted more than 16 h after injection, whereas the tumors injected with siAIB1 alone exhibited no fluorescence since 8 h after injection. It is speculated that the Ca^{2+}/PEI/Heparin NPs packaged FAM-siAIB1 prevent nonspecific protein adsorption and aggregation of the nanoparticles in tumor tissues, thus Ca^{2+}/PEI/Heparin NPs/FAM-siAIB1 accumulated at the tumor site for a longer time than siRNA alone.

CLSM images (Figure 8b) of Tumor frozen slices which was stained with DAPI at 16 h post injection show the distribution of FAM-siAIB1 in tumor following intratumoral injection of PBS solution, FAM-siAIB1 only and Ca^{2+}/PEI/Heparin NPs/FAM-siAIB1, confirming remanence of FAM-siAIB1 in Ca^{2+}/PEI/Heparin NPs group rather than in control groups upon animal sacrifice.

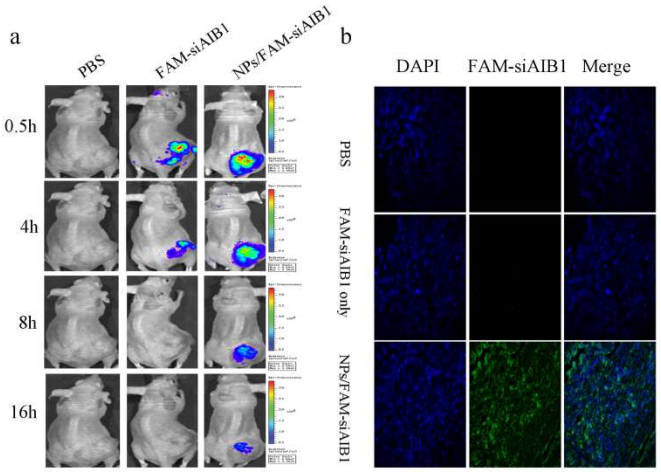

Figure 8. *In vivo* Ca^{2+}/PEI/Heparin NPs complexes transfection and fluorescence imaging. (a) Fluorescence images of MCF-7 xenograft-bearing mice after intratumoral injection of PBS, FAM-siAIB1 or Ca^{2+}/PEI/Heparin NPs (NPs/FAM-siAIB1). (b) Fluorescence images of tumors at 16 h post intratumoral injection of PBS solution, FAM-siAIB1 only and NPs/FAM-siAIB1. FAM-siAIB1 was labled in green. Cell nuclei were stained with DAPI (blue).

Tumor suppression study and expression levels of NF-κB and BCL-2 in tumor tissues

We examined the anti-tumor growth effect of Ca^{2+}/PEI/Heparin NPs/siAIB1 *in vivo*. Athymic mice bearing MCF-7 cell xenografts received a weekly intratumoral injection of 20 μg Ca^{2+}/PEI/Heparin NPs/siAIB1 for 5 times (Figure 9a). As shown in Figure. 9b-d, intratumoral injection of Ca^{2+}/PEI/Heparin NPs/siAIB1 significantly inhibited the tumor growth (23.5 ± 6.1 v/v% and 7.8 ± 2.6 wt% of volume/weight reduction), whereas injection of siAIB1 alone also show a weak tumor volume reduction of 86.9 ± 9.8% (Figure. 9b) and a tumor weight reduction of 87.8 ± 13.2% (Figure. 9c).[23] The results suggest that localized siRNA delivery by intratumoral injection of Ca^{2+}/PEI/Heparin NPs/siAIB1 complexes can efficiently inhibit breast cancer cells growth *in vivo*.

To further explore the mechanisms underlying the anti-tumor growth effect mediated by Ca^{2+}/PEI/Heparin NPs/siAIB1, the downstream signaling pathway of AIB1 was investigated. It has been suggested that knockdown of AIB1 protein by siRNA level in human chronic myeloid leukemia K562 cells leads to apoptosis via inactivation of NF‐κB signaling,[24] while overexpression of AIB1 in human embryonic kidney 293 cells reverses this effect.[25] Thus, we analyzed the protein expression of the NF-κB and BCL-2 in the subcutaneous tumor tissues by western blotting. Consistent with the change of AIB1 protein, NF-κB and BCL-2 protein levels were markedly decreased in the tumors injected with Ca^{2+}/PEI/Heparin NPs/siAIB1 (Figure 9e), indicating that NF-κB/BCL-2 signal pathway might be the downstream signal pathway of AIB1 in regulating breast cancer proliferation and progression.

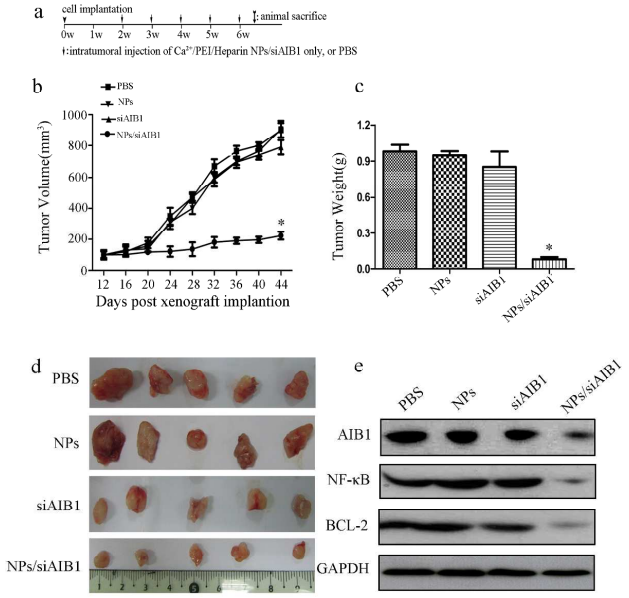

Figure 9. Intratumoral injection of Ca^{2+}/PEI/Heparin NPs complexes inhibited tumor growth. (a) The timeline for *in vivo* antitumor activities assessment of Ca^{2+}/PEI/Heparin NPs complexes in a subcutaneous xenograft model. (b) Growth curve of mean tumor size in nude mice injected with PBS, NPs, siAIB1 or Ca^{2+}/PEI/Heparin NPs/siAIB1 (NPs/siAIB1). Data shown were obtained from three independent experiments and are presented as the means ± SD. *$P < 0.05$ vs PBS. (c) Mean tumor weights at 30 days after the first injection. (d) Actual sizes of representative tumors. (e) Western blotting analysis of the expression levels of NF-κB and BCL-2 in each group. GAPDH was used as a loading control.

To further explore if injection methods of Ca^{2+}/PEI/Heparin NPs/siAIB1 would affect the transfection efficiency, athymic mice bearing MCF-7 cell xenografts received a weekly intravenous injection of 20 μg Ca^{2+}/PEI/Heparin NPs/siAIB1 for 5 times. As shown in Figure.10b-d, intravenous injection of Ca^{2+}/PEI/Heparin NPs/siAIB1 did not increase tumor volume and weight significantly compared with control group. The results suggest that localized siRNA delivery by intravenous injection of Ca^{2+}/PEI/Heparin NPs/siAIB1 complexes can efficiently inhibit breast cancer cells growth *in vivo*. Besides, NF-κB and BCL-2 protein levels were markedly decreased in the tumors injected with Ca^{2+}/PEI/Heparin NPs/siAIB1 (Figure 10e), further confirm the involvement of the NF-κB/BCL-2 signal pathway in regulating breast cancer proliferation and progression.

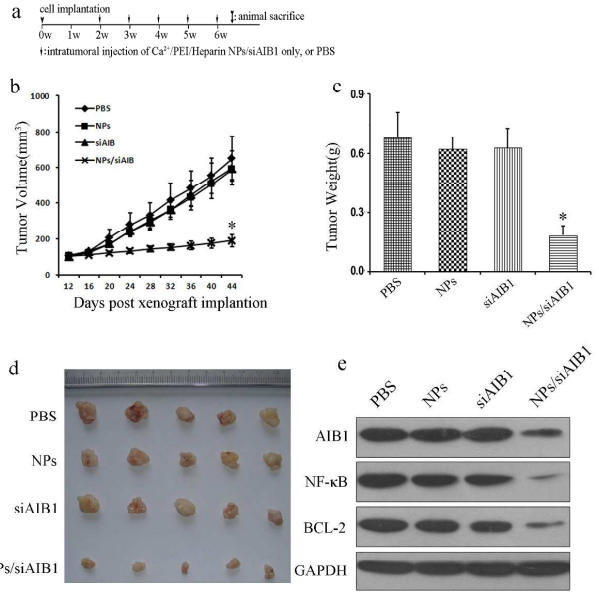

Figure 10. Intravenous injection of Ca^{2+}/PEI/Heparin NPs complexes inhibited tumor growth. (a) The timeline for *in vivo* antitumor activities assessment of Ca^{2+}/PEI/Heparin NPs complexes in a subcutaneous xenograft model. (b) Growth curve of mean tumor size in nude mice injected with PBS, NPs, siAIB1 or Ca^{2+}/PEI/Heparin NPs/siAIB1 (NPs/siAIB1). Data shown were obtained from three independent experiments and are presented as the means ± SD. *$P < 0.05$ vs PBS. (c) Mean tumor weights at 30 days after the first injection. (d) Actual sizes of representative tumors. (e) Western blotting analysis of the expression levels of NF-κB and BCL-2 in each group. GAPDH was used as a loading control.

Experimental

Cell culture and reagents

Human breast tumor cell lines MCF-7, SK-BR-3 and MAD-MB-231 obtained from ATCC was cultured in Dulbecco's modified Eagle's medium (Cellgro; Manassas VA, USA) supplemented with 10% fetal bovine serum (Cellgro; Manassas VA, USA) at 37°C with 5% CO_2. The heparin sodium and $CaCl_2$ were obtained from Aladdin (Shanghai, China). Branched PEI with a weight-averaged molar mass of 25,000 g/mol (BPEI 25 kDa) was obtained from Sigma-Aldrich (St. Louis, MO, USA).

Synthesis and characterization of Ca^{2+}/PEI/Heparin NPs

Ca^{2+}/PEI/Heparin NPs were prepared in a standard synthetic route. $CaCl_2$ (2 mL, 22 mg/mL) aqueous solution, PEI (1 mL, 32 mg/mL) solution and heparin sodium (500 μL, 32 mg/mL) were mixed in a 25 mL glass beaker with addition of 17 mL double distilled water. The mixture was stirred at room temperature for 24 h. The white

Ca^{2+}/PEI/Heparin precipitates were collected by centrifugation at 9000 rpm for 3 min, washed with double distilled water and dried at 40°C under vacuum overnight. Scanning electron microscopic (SEM) images were taken with a JEOL JSM-6700F operated at 15 kV. Fourier transform infrared (FTIR) spectra were recorded on a Nicolet Nexus spectrometer with samples embedded in KBr pellets. Energy dispersive X-ray spectroscopy (EDS) spectrum was obtained on a JEOL-2010 microscope with an accelerating voltage of 200 kV.

Gel retardation assay and MTT assay

The complex formation of siRNA with Ca^{2+}/PEI/Heparin NPs was analyzed by agarose gel electrophoresis. The Ca^{2+}/PEI/Heparin NPs and siRNA were mixed at the mass ratio of 100:1, 50:1, 30:1, 10:1, and 1:1. Then the Ca^{2+}/PEI/Heparin NPs/siRNA complexes were left at room temperature for 30 min to facilitate the complexation. The samples were centrifuged at 5,000 rpm for 5 min, followed by agarose gel electrophoresis. The suspensions were loaded into 1% agarose gels prestained with ethidium bromide (EtBr, 0.1 μg/mL) and run at 100 V for 40 min in Tris-acetate (TAE) buffer (0.045 M TAE; 0.001 M EDTA). The bands were visualized by a UV transilluminator.

For MTT assay, MCF-7 cells were seeded in 96-well plates at a density of 8×10^3 cells per well and transfected with 50 nM siNC complexed with different concentrations of Ca^{2+}/PEI/Heparin NPs (1 mg/mL, 50 mg/mL, 100 mg/mL, and 150 mg/mL), 50 nM siNC by Lipofectamine 2000, the siNC only, 50 nM Ca^{2+}/PEI/Heparin NPs only, or phosphate-buffered saline. After transfection, cells were cultured at 37°C with 5% CO_2 for 4 days. Then the medium was replaced with 100 μL fresh medium, and 20 μL of 5 mg/mL MTT was added to each well. The cell cultures were incubated for 4 h, and the medium was replaced again. Then 150 μL of dimethyl sulphoxide (DMSO) was added to each well. Plates were shaken at 600 r/min for 10 min. The optical density (OD) was measured at 490nm using a microplate spectrophotometer.

***In vitro* transfection and the distribution of Ca^{2+}/PEI/Heparin NPs /FAM-siAIB1**

In vitro transfection was performed as described previously. In brief, cells were cultured in three 24-well plates at a density of 5×10^4 cells per well and grew overnight to achieve 60-80% confluence. The cells were transfected with siRNA by using Ca^{2+}/PEI/Heparin NPs or Lipofectamine 2000. The Lipofectamine 2000 transfection kit (Invitrogen, Carlsbad, CA) was used following the manufacturer's protocol. The siRNA specific for human AIB1 (siAIB1) (GenBank accession) and the negative control siRNA (siNC) were purchased from Qiagen (Valencia, CA).

The sequences of siAIB1 were 5'-r(GGUGAAUCGAGACGGAAAC)dTT-3' and 5'-r(GUUUCCGUCUCGAUUCACC)dTTT-3'. The sequences of siNC were 5'-r(UCCGUUUCGGUCCACAUUC)dTT-3 and 5'-r(GAAUGUGGACCGAAACGGA)dTT-3' Fluorescein-tagged siRNA (FAM-siRNA) was synthesized by labeling the 3'-end of the sense strand of the siAIB1 with fluorescein. After 6 h, transfect efficiency were analyzed by inverted fluorescence microscope (Olympus, IX71, Japan). Then the cells were trypsinized, collected by centrifuged at 2,000g for 3 min, and resuspended in phosphate-buffered saline. Then the cells were subjected to flow cytometry analysis (Beckman Coulter).

For confocal laser scanning microscopy (CLSM) observations, MCF-7 cells (5×10^4 cells/well) were seeded in a 35 mm glass bottom culture dish (MatTek Corporation) and incubated at 37°C with 5% CO_2 for 24 h. Then the cell culture medium were replaced with Ca^{2+}/PEI/Heparin NPs/FAM-siAIB1 complexes in 500 μL serum free RPMI 1640 culture medium for each well. At predetermined time intervals, the cells were washed 3 times with the phosphate-buffered saline. The nucleis were stained with DAPI (4',6'-diamidino-2-phenylinodole, Sigma) for 5 min. Then the cells were directly observed under the Olympus FluoView confocal microscopes and analyzed with FV10-ASW viewer software (Olympus, Tokyo, Japan).

Analysis of AIB1 expression

MCF-7 cells (5×10^4) were cultured in 24-well plates and incubated at 37°C with 5% CO_2 for 24 h to reach about 70% confluence. Ca^{2+}/PEI/Heparin NPs/siAIB1 (50 nM or 100 nM or 150 nM of siAIB1, 50:1 mass ratio), equivalent amount of Ca^{2+}/PEI/Heparin NPs/siNC (150 nM siNC), Ca^{2+}/PEI/Heparin NPs, or phosphate-buffered saline were added and incubated with the cells for 24 h before mRNA isolation or 48 h before protein extraction.

The expression of AIB1 mRNA was analyzed by real time PCR assay. Total RNA was extracted with TRIzol reagent (Invitrogen, Carlsbad, California, USA) and reverse transcribed into cDNA using the PrimeScript RT reagent Kit (Promega, Madison, WI, USA). The ABI 7900HT fast RT-PCR system and relative quantification software (Applied Biosystems, Foster City, California, USA) were used for real-time analyses. Amplification consisted of 30 cycles of 30 s at 94°C, 30 s at 55°C and 60 s at 72°C. The amplification for real time PCR used the following primers and probes: AIB1 forward primer, 5'-CAGTGATTCACGAAAACGCA-3'; AIB1 reverse primer, 5'-CAGCTCAGCCAATTCTTCAAT-3'; AIB1 probe, 6FAM-TGCCATGTGATACTCCAGAAG-BHQ1; GAPDH forward primer, 5'-CCCACATGGCCTCCAAGGAGTA-3'; GAPDH reverse primer, 5'-GTGTACATGGCAACTGTGAGGAGG-3'; and GAPDH probe, 6FAM-ACCCCTGGACCAGCCCCAGC-TAMRA.

For Western blotting, whole-cell or tissues lysates were prepared by Laemmli Sample Buffer. Samples were separated by sodium dodecyl sulfate polyacrylamide gel electrophoresis, and proteins were transferred onto polyvinylidene difluoride membranes (Pall Corp., Port Washington, NY). Mouse anti-AIB1, anti-NF-κB, anti-Bcl-2, and anti-GAPDH antibodies (Abcam, Cambridge, UK) were used for Western blotting and immunohistochemistry. After the blocking, membranes were incubated in the appropriate dilution of primary antibodies in 5% milk in PBST at room temperature for 1 h. Blots were washed three times for 5–10 min per wash in 1 × TBST followed by incubation in the appropriately diluted secondary antibodies at room temperature for 1 h. The blots were washed three times in 1 × TBST for 5 min. Enhanced chemiluminescence detection reagents (Amersham Biosciences, Uppsala, Sweden) was used for antigen detection.

Cell proliferation, apoptosis, and cell cycle analyses after siAIB1 transfection

Cell proliferation was determined by MTT assay. MCF-7 cells were cultured in 96-well plates at a density of 8×10^3 cells per well. After transfection for 24, 48, 72, 96, 120, and 144 h, 20 μL of MTT (Sigma-Aldrich) solution (5 mg/mL) was added into each well and incubated for 4 h. Then, the reaction was terminated by removing all medium and adding 150 μL of DMSO. The optical density (OD) was measured at 490 nm using a microplate spectrophotometer.

Apoptosis analysis was performed by using the Annexin V apoptosis detection kit (BD biosciences). Following manufacture's protocol, MCF-7 cells were stained with annexin V-PE and propidium iodide (PI) 48 h after transfection. The percentage of apoptotic cells was quantified by flow cytometry. Both Annexin V-PE and PI negative cells are considered as viable.

For cell cycle analysis, MCF-7 cells were cultured in a 24-well plate at a density of 5×10^4 cells/well. Forty-eight hours after transfection, cells were trypsinized and fixed by 70% ethanol and stained by using a Coulter DNA-Prep Reagents kit (Beckman Coulter, Fullerton, CA). Cellular DNA content from each sample was measured with flow cytometry (Becton Dickinson, San Jose, CA, USA).

In vivo fluorescence imaging

For *in vivo* imaging, 400 μL of Ca^{2+}/PEI/Heparin NPs/FAM-siAIB1, FAM-siAIB1, or phosphate-buffered saline were injected intratumorally in female MCF-7 tumor-bearing mice model. Mice were placed on a warmed stage inside of an IVIS light-tight chamber, and anesthesia was maintained with 2.5% isoflurane throughout the imaging session. Images were acquired at different time intervals with Xenogen IVIS Lumina system (Caliper Life Sciences, USA) and analyzed by Living Image 3.1 software (Caliper Life Sciences, USA).

Tumor suppression study *in vivo*

BALB/c nu/nu immune deficient mice (6 weeks old, 18-20 g) were purchased from Shanghai Slac Laboratory Animal Co., Ltd. (Shanghai, China). After a monolayer of MCF-7 cells was formed, a single cell suspension of these cells was prepared using the trypsin digestion method. The cells were adjusted to a concentration of 4×10^7 in 100 μL of phosphate-buffered saline and injected subcutaneously into the right flank of each mouse. Once the MCF-7 cells developed a tumor with a volume about 100 mm^3, Ca^{2+}/PEI/Heparin NPs/siAIB1 (20 μg of siAIB1 per injection, 50:1 at mass ratio), equivalent amount of Ca^{2+}/PEI/Heparin NPs, siAIB1 only, or phosphate-buffered saline were injected directly into the tumors. To investigate the transfection efficiency in groups using different injection methods, Ca^{2+}/PEI/Heparin NPs/siAIB1 (20 μg of siAIB1 per injection, 50:1 at mass ratio), equivalent amount of $^{Ca2+/}$PEI/Heparin NPs, siAIB1 only, or phosphate-buffered saline were injected intravenously into the mouse. The long and short axial lengths of the tumors were measured every other day. Mice were sacrificed 30 days after the first injection and tumor samples were collected for further analyses.

Ethical standards

All animal studies were conducted in accordance with the Guide for Care and Use of Laboratory Animals as adopted and promulgated by the United National Institutes of Health and were approved by the Institute Research Medical Ethics Committee of Sun Yat-sen University.

Statistical analysis

All experiments were repeated at least three times. Data are reported as means±standard deviation. Statistical significance was evaluated by using Student's t-test, when only two groups were compared. If more than two groups were compared, evaluation of significance was performed using ANOVA followed by Bonferroni's post hoc test. In all tests, $P<0.05$ was considered significant.

Conclusions

We developed Ca^{2+}/PEI/Heparin nanocomposite particles that can efficiently load siRNA and transfect it into human breast cancer cells without obvious cytotoxicity. The interaction between PEI and heparin greatly reduces the cytotoxicity of 25 kDa PEI, and the addition of Ca^{2+} results in nanosized Ca^{2+}/PEI/Heparin particles. The nanoparticles can efficiently deliver siRNA into cells, facilitate the escape of loaded siRNA from the endosome into the cytoplasm, downregulate the target gene and consequently inhibit cancer cell growth *in vitro*. Furthermore, the nanoparticles carrying siAIB1 exhibit good penetrability and ability to protect siRNA from degradation in tumor tissues. Intratumoral and intravenous injection of Ca^{2+}/PEI/Heparin NPs/siAIB1 complexes inhibits breast tumor growth in xenograft murine model, likely by downregulation of AIB1 and the NF-κB/BCL-2 signaling pathway. All of these results suggest that the Ca^{2+}/PEI/Heparin NPs may serve as a novel and effective siRNA delivery carrier for cancer therapy.

Acknowledgements

This work was supported by the National Basic Research Program of China (2010CB934700) and the National Natural Science Foundation of China (30900539, 81172429, 81372821).

Notes

[a]Department of Breast Surgery, First Affiliated Hospital, Sun Yat-Sen University, Guangzhou, 510080, China;

[b] Department of Chemistry, Tongji University, Shanghai 200092, China;

[c] Department of Vascular Surgery, First Affiliated Hospital, Sun Yat-Sen University, Guangzhou, 510080, China;

[d] Department of Neurological Intensive Care Unit, First Affiliated Hospital, Sun Yat-Sen University, Guangzhou, 510080, China;

[e] Department of Urology, First Affiliated Hospital, Sun Yat-Sen University, Guangzhou, 510080, China;

[f] Division of Nanomaterials and Chemitry, Hefei National Laboratory for Physical Sciences at Microscale, University of Science and Technology of China, Hefei, 230026, China;

[#]These authors contributed equally to this work.

[*] Correspond to:

S.M Wang: shenmingwang@vip.sohu.com; Y. Lin: frostlin@hotmail.com;A.W Xu: anwuxu@ustc.edu.cn;Tel: +86 133 0222 4168, Fax: +86 20 8775 5766.

References

[1] F. Tang, J. A. Hughes, *Methods Mol Med*,2001,**65**,79-88.

[2] S. D. Li, L. Huang, *J Control Release*,2007,**123**,181-183.

[3] A. Gautam, C. L. Densmore, E. Golunski, B. Xu, J. C. Waldrep, *Mol Ther*,2001,**3**,551-556.

[4] W. T. Godbey, K. K. Wu, A. G. Mikos, *J Control Release*,1999,**60**,149-

160.

[5] R. Kircheis, A. Kichler, G. Wallner, M. Kursa, M. Ogris, T. Felzmann, M. Buchberger, E. Wagner, *Gene Ther*,1997,**4**,409-418.

[6] M. Ogris, S. Brunner, S. Schuller, R. Kircheis, E. Wagner, *Gene Ther*,1999,**6**,595-605.

[7] C. Brunot, L. Ponsonnet, C. Lagneau, P. Farge, C. Picart, B. Grosgogeat, *Biomaterials*,2007,**28**,632-640.

[8] S. M. Moghimi, P. Symonds, J. C. Murray, A. C. Hunter, G. Debska, A. Szewczyk, *Mol Ther*,2005,**11**,990-995.

[9] P. Tryoen-Toth, D. Vautier, Y. Haikel, J. C. Voegel, P. Schaaf, J. Chluba, J. Ogier, *J Biomed Mater Res*,2002,**60**,657-667.

[10] D. Goula, C. Benoist, S. Mantero, G. Merlo, G. Levi, B. A. Demeneix, *Gene Ther*,1998,**5**,1291-1295.

[11] R. Kircheis, S. Schuller, S. Brunner, M. Ogris, K. H. Heider, W. Zauner, E. Wagner, *J Gene Med*,1999,**1**,111-120.

[12] F. Zhao, M. L. Ma, B. Xu, *Chem Soc Rev*,2009,**38**,883-891.

[13] C. M. Lehman, E. L. Frank, *Lab Medicine*,2009,**40**,47-51.

[14] L. Josephson, C. H. Tung, A. Moore, R. Weissleder, *Bioconjug Chem*,1999,**10**,186-191.

[15] J. F. Liang, Y. T. Li, H. Song, Y. J. Park, S. S. Naik, V. C. Yang, *J Control Release*,2002,**78**,67-79.

[16] J. F. Liang, H. Song, Y. T. Li, V. C. Yang, *J Pharm Sci*,2000,**89**,664-673.

[17] C. Hu, L. Zhang, D. Wu, S. Cheng, X. Zhang, R. Zhuo, *Journal of Materials Chemistry*,2009,**19**,3189-3197.

[18] M. C. Martins, S. A. Curtin, S. C. Freitas, P. Salgueiro, B. D. Ratner, M. A. Barbosa, *J Biomed Mater Res A*,2009,**88**,162-173.

[19] N. Morimoto, A. Watanabe, Y. Iwasaki, K. Akiyoshi, K. Ishihara, *Biomaterials*,2004,**25**,5353-5361.

[20] J. Wei, T. Cheang, B. Tang, H. Xia, Z. Xing, Z. Chen, Y. Fang, W. Chen, A. Xu, S. Wang, J. Luo, *Biomaterials*,2013,**34**,1246-1254.

[21] D. Fischer, T. Bieber, Y. Li, H. P. Elsasser, T. Kissel, *Pharm Res*,1999,**16**,1273-1279.

[22] Y. X. Tan, C. Chen, Y. L. Wang, S. Lin, Y. Wang, S. B. Li, X. P. Jin, H. W. Gao, Du FS, F. Gong, S. P. Ji, *J Gene Med*,2012,**14**,241-250.

[23] G. Zhou, Y. Hashimoto, I. Kwak, S. Y. Tsai, M. J. Tsai, *Mol Cell Biol*,2003,**23**,7742-7755.

[24] G. P. Colo, R. R. Rosato, S. Grant, M. A. Costas, *FEBS Lett*,2007,**581**,5075-5081.

[25] G. P. Colo, M. F. Rubio, I. M. Nojek, S. E. Werbajh, P. C. Echeverria, C. V. Alvarado, V. E. Nahmod, M. D. Galigniana, M. A. Costas, *Oncogene*,2008,**27**,2430-2444.